Proceeding of the IEEE
International Conference on Robotics and Biomimetics
Dali, China, December 2019

A Full Span Magnetic Localization Algorithm

Chao Hu, Zhihuan Zhang, Jun Qiu, Yupeng Ren
Ningbo Institute of Technology, Zhejiang University, Ningbo, China; huchao@nit.net.cn

Houde Dai
Quanzhou Institute of Equipment Manufacturing, Haixi Institutes, Chinese Academy of Sciences, Jinjing, China

Shuang Song
Shenzhen Graduate School, Harbin Institute of Technology, Shenzhen, China *Department of Intelligent Robotics*

Wanan Yang
School of Computer and Information, Yibin University. Yibin, China

***Abstract* - Magnetic dipole is a conventional model for the localization of a magnet. However, a restriction is that the distance from the test field point to the magnet's position must be long enough comparing with the length of the magnet. Otherwise, the dipole model is inaccurate, which is known as the near-field problem. In this paper, we investigated the near-field magnetic density distribution for a circular ring magnet with respect to the magnet's center, which is simply symmetrical about the magnet's main axis, so it is in 2 dimensions. Further, we propose the full span (including near-field) localization algorithm on this distribution, which minimizes the calculation error between the measured flux densities and those calculated from the spatial and rotation transforms from the global coordinate system to the magnet's coordinate system, so as to compute the magnetic density on the 2D field density distribution. Simulation results show that the proposed method can accurately to obtain the magnet's position and orientation in near-field.**

***Index Terms* - Magnetic Dipole, Near-field Distribution, Full Span Magnetic Localization.**

I. Introduction

Magnet-based localization has the advantages of power-free, small space occupying, and easy setting up. So it has been caught great attention of the researchers in the tracking of the indoor objectives, such as the localization of the indoor robots [1] and the intra-body objectives for medical applications [2-4], especially used for the capsule endoscopy [5, 6]. Typically, this localization is based on the assumption that magnetic field built by a magnet can be modelled as a magnetic dipole. If there are enough magnetic sensors arranged around the magnet to detect its magnetic flux signals, the magnet's position and orientation can be computed by applying linear [7] or nonlinear algorithms [8] on the known mathematic model.

However, one problem is that such a dipole model is not accurate when the field point (or the sensor position) is too close to the magnet, which is known as the near-field problem [9]. Thus, it is desirable to find an improved localization approach to enhance the localization accuracy. One method to solve this problem is to apply the integration computation for the magnetic flux. However, since there are 6 (3 position and 3 orientation) parameters (*a, b, c, m, n, p*) for locating a moving magnet as shown in Fig.1, it is difficulty to directly compute the flux distribution with all the 6 parameters. Here, we propose a novel method that is on the magnetic flux distribution with respect to the circular magnet's center. Obviously, this distribution is simply symmetrical about the magnet's main axis $\mathbf{H_0}$, so it is in 2 dimensions (2D). We can find this 2D distribution through the digital integration calculation or through the real experiments in advance, and build a 2D relationship (e.g. 2D lookup table) for the magnetic flux densities. In real localization, a coordinate transform is applied from global coordinate system of XYZ to that of X'Y'Z' where the Z'-axis is the same as the magnet's main axis, and in this X'Y'Z' system the magnetic flux densities in the all sensors' positions can be computed by the 2D distribution relationship. Further, these magnetic flux densities are transformed reversely to the XYZ coordinate system, and compared with the measurements of the real sensors. Recursions are made to have this comparison error to the minimum, and the final solution for the near-field localization is realized.

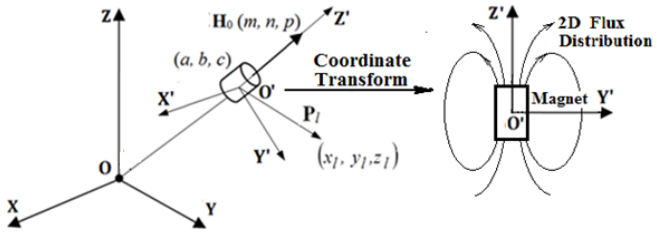

Fig.1 Magnet's localization model & its coordinate transform

The organization of the rest of the paper is as follows. In section II, we discuss the dipole model and its localization. In section III, we present the near-field model and its evaluation. In section IV, we propose the near-field localization algorithm. In section V, we present the simulation results, followed by the conclusion in section VI.

II. Magnetic Dipole Model & Its Localization

For a magnet's localization, if the size of the magnet is small enough relative to the detection distance, the magnet can be modelled as a magnetic dipole, defined by equation (1). As shown in Fig.1, $P_l(=[x_l - a, y_l - b, z_l - c]^T)$ is defined as the displacement vector from a spatial position (x_l, y_l, z_l) with respect to the magnet center (*a, b, c*), where *l*=1, 2… N, representing the sensor number. R_l is the module of P_l. The magnetic flux density B_l in (x_l, y_l, z_l) is defined as

978-1-7281-6321-5/19//$31.00 ©2019 IEEE

$[B_{lx}\ B_{ly}\ B_{lz}]$, the three orthogonal components of the magnetic flux density; μ_r is the relative permeability and μ_0 the vacuum permeability ($\mu_0 = 4\pi \times 10^{-7}$ T·m/A); M_T defines the constant of the magnet's density related to its volume and magnetized intensity $\mathbf{H}_0$ ($=[m, n, p]^T$) is the orientation vector of the magnet's main axis. Because the rotation around the circular magnet's main axis does not change the magnetic field distribution, the effective DOF of the orientation is in 2 dimensions; and the orientation vector is constrained to be unity as (2)

$$\begin{aligned}\mathbf{B}_l &= B_{lx}\mathbf{i} + B_{ly}\mathbf{j} + B_{lz}\mathbf{k} \\ &= \frac{\mu_r \mu_0 M_T}{4\pi}\left(\frac{3(\mathbf{H}_0 \cdot \mathbf{P}_l)\mathbf{P}_l}{R_l^5} - \frac{\mathbf{H}_0}{R_l^3}\right) \\ &= B_T\left(\frac{3(\mathbf{H}_0 \cdot \mathbf{P}_l)\mathbf{P}_l}{R_l^5} - \frac{\mathbf{H}_0}{R_l^3}\right) \quad (l=1, 2, \cdots, N)\end{aligned} \tag{1}$$

$$m^2 + n^2 + p^2 = 1 \tag{2}$$

The magnetic flux intensities B_{lx}, B_{ly}, and B_{lz} can be measured by magnetic sensors corresponding to the XYZ coordinates; and the magnet's position and orientation can be computed by above equations (1)~(2).

For example, a linear localization algorithm was proposed in [7]. Making the cross product with $\mathbf{P}_l$ on both sides of (1) and then dot product with $\mathbf{H}_0$, we have

$$(\mathbf{B}_l \times \mathbf{P}_l) \cdot \mathbf{H}_0 = 0 \qquad (l=1,2,\ldots N) \tag{3}$$

That is

$$\begin{pmatrix} B_{lx} \\ B_{ly} \\ B_{lz} \end{pmatrix} \times \begin{pmatrix} x_l - a \\ y_l - b \\ z_l - c \end{pmatrix} \cdot \begin{pmatrix} m \\ n \\ p \end{pmatrix} = 0 \qquad (l=1,2,\ldots N) \tag{4}$$

Then, we get

$$[B_x, B_y, B_z, (B_z y_l - B_y z_l), (B_x z_l - B_z x_l)] \begin{bmatrix} b - cn' \\ cm' - a \\ an' - bm' \\ m' \\ n' \end{bmatrix} = B_x y_l - B_y x_l \tag{5}$$

Where $m' = m/p$, $n' = n/p$. Define

$$\begin{aligned}\mathbf{F}_l &= [f_{l1}, f_{l2}, f_{l3}, f_{l4}, f_{l5}] \\ &= [B_x, B_y, B_z, (B_z y_l - B_y z_l), (B_x z_l - B_z x_l)]\end{aligned} \tag{6}$$

$$u_l = B_{lx} y_l - B_{ly} x_l , \tag{7}$$

$$\mathrm{R} = [(b - cn'), (cm' - a), (an' - bm'), m', n']^T \tag{8}$$

With 5 sensors we can solve

$$\mathbf{R} = \mathbf{M}^{-1}\mathbf{U} \tag{9}$$

Where $\mathbf{M} = [\mathbf{F}_1\ \mathbf{F}_2\ \mathbf{F}_3\ \mathbf{F}_4\ \mathbf{F}_5]^T$ and $\mathrm{U} = [u_1\ u_2\ u_3\ u_4\ u_5]^T$.

Provided there are totally N(>5) three-axis sensors, we change the expression of (5), and define the fitting error to be $\Delta E = \sum_{l=1}^{N} [\mathbf{F}_l \mathrm{R} - u_l]^2$. The optimal solution of R making ΔE minimum is

$$\mathrm{R} = \mathbf{M}_B^{-1}\mathrm{U}_S \tag{10}$$

Where $\mathrm{M_B}$ is a 5×5 matrix, in which the *i*th row and *j*th column element is $m_{ij} = \sum_{l=1}^{N} f_{li} \cdot f_{lj}$ (i=1…5; j=1…5; N>5) with f_{li} and f_{lj} given by (6); $\mathbf{U}_S$ is a vector, in which the *i*th element is $\hat{u}_i = \sum_{l=1}^{N} u_{1l} \cdot f_{li}$ (i=1…5; N>5) with u_l given by (7). With the solution $\mathrm{R} = [(b - cn'), (cm' - a), (an' - bm'), m', n']^T$, we can further solve for the position and orientation parameters (*a, b, c, m, n, p*) of the objective magnet.

However, a problem for above algorithm is that the dipole model is not accurate in the near-field, where the field point (the test position) is too close to the magnet, and R_l is not long enough compared with the length (or the size) of the magnet. In order to find more accurate model, we investigated the magnet's field distribution on the simulations and experiments. Further, a novel method proposed to realize the magnet's near-field localization.

III. Near-Field Model & Its Evaluation

3.1 Experiments

The experiments were done on an axially magnetized ring magnet (16mm in length, 6mm in radius, and 1.5mm in thickness) , as shown in Fig.2. The magnet is fixed in the origin of the coordinate system. The magnetic flux density is measured from -6cm to +6cm in Y coordinate with the interval 0.5cm, and from +3.15cm to +14.15cm in Z coordinate. The measured flux density along the vertical axis is denoted as B'_{lz}, and is shown in Fig.3(a). The errors between measured values and those in dipole model are shown in Fig.3(b). The mean error value is 0.0168mT; and the error in the closest point (0, 3.15) is 0.2872mT, about 5.5% of the flux density in this position.

3.2 Computing the flux density of a ring magnet

The magneto motive force in a spatial point around the permanent magnet can be defined as a scalar:

$$\varphi_m = \frac{1}{4\pi}\oint_S \frac{\rho_{sm}}{R} dS + \frac{1}{4\pi}\oint_\tau \frac{\rho_{sm}}{R} d\tau \qquad (11)$$

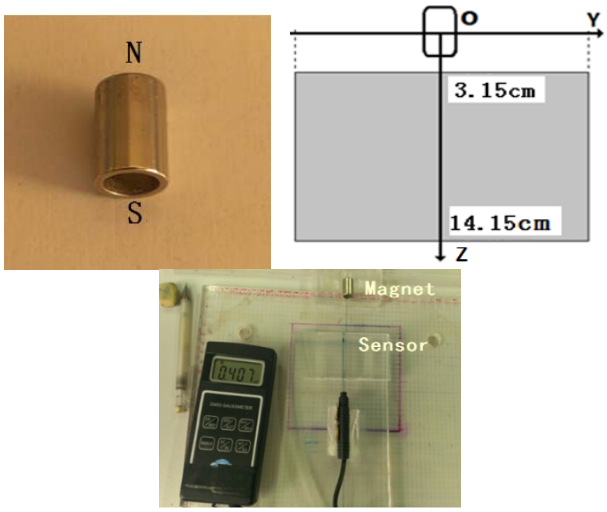

Fig. 2 Measure the magnetic strength of the Ring Magnet

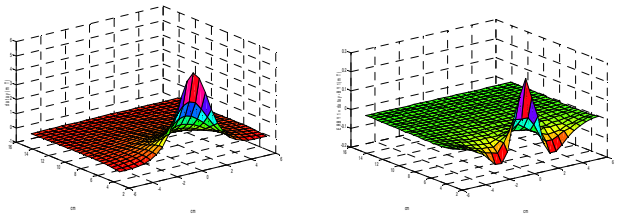

(a) Flux Density Distribution (b) Error Distribution vs. dipole

Fig. 3 Measurements of axial magnetic flux density of a ring magnet

Where, ρ_{sm} and ρ_m are surface density and volume density of the magnet; S is the surface enclosing the magnet; τ is the volume of the magnet; R is the distance from the source point to the field point. The magnetic flux density is the gradient on the magneto motive force. Because the common permanent magnet has no magnetic charge inside and the magnetic charges only exist on the top and bottom surfaces, the magnetic flux density can then be derived as

$$\mathbf{B} = \frac{\mu_0\mu_r}{4\pi}\oint_S \nabla\frac{\rho_{sm}}{R} dS = \frac{\mu_0\mu_r\rho_{sm}}{4\pi}\oint_S \frac{\mathbf{P}}{R^3} dS \qquad (12)$$

where **P** represents the vector from the source point to the field point. Here, we propose a numerical integration method to compute the flux density specifically for a ring magnet. As shown in Fig.4, the main axis of the magnet is along the Z-axis; A_1 and A_2 are the paired small elements of the top (N) and bottom (S) surface areas of the ring magnet, positioned in (a_1, b_1, w) and (a_1, b_1, -w). Thus the magnetic flux density can be calculated by

$$\mathbf{B} = \frac{\mu_0\mu_r M_T}{8\pi^2}\int_0^{2\pi}\left(\frac{\mathbf{P}_1}{R_1^3} - \frac{\mathbf{P}_2}{R_2^3}\right)d\theta \qquad (13)$$

Where R_1=|P$_1$|; R_2=|P$_2$|; $M_T = \rho_{sm} S_m$, defines the constant of the magnet's density relative to the surface density ρ_{sm} and the surface area S_m.

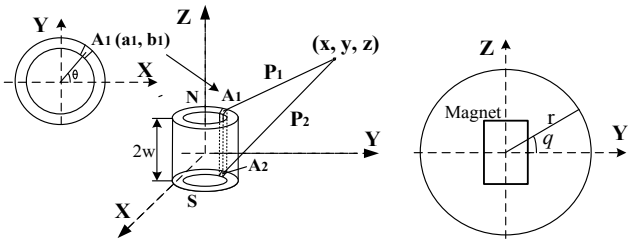

Fig.4 Spatial Relation of Ring Magnet

3.3 Near-field model vs. dipole model

The field density of the ring magnet is calculated by the integration (13), where the ring is circularly divided into 16 elements while the source point is assumed in the centre in each element. Fig.5 shows the relative errors of axial magnetic intensity B_z (Z-axis) comparing with those of the dipole when field point changes with Y-coordinates while fixing (X, Z) coordinates in (0, 3.15cm). We observe the error curve much alike to the error curve of the measured values (by experiment) in Fig. 3(b).

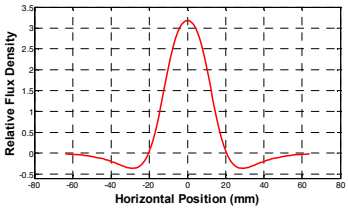

Fig.5 Axial density errors between integrations to the dipole in (0, Y, 3.15cm)

One concerned issue is how much the distance of the field point relative to the magnet's length is required for the magnet to be modelled as a magnetic dipole. To examine this, we set up field points along the circles with different radius ***r*** around the magnet, as shown in Fig.4(b), and computed the differences for the integration model vs. the dipole. Because the ring magnet's field is symmetrical along its main axis, we examine the magnetic field on the YZ-plane with X-coordinate fixed to be zero, while the field point (0, $r\cdot\cos\boldsymbol{\theta}$, $r\cdot\sin\boldsymbol{\theta}$) changing along the circle. Fig.6 shows the resulted magnetic densities B_y and B_z in the field points with radius ***r***=20mm. Fig.7 shows the those with radius ***r***=15mm, and we observed that the differences are much larger for the latter case. Fig.8 shows relative percentage errors of the magnetic flux density to the dipole in different radii, which is given by

$$\Delta R_B = \frac{\sqrt{\sum_{j=1}^{N}\left|\mathbf{B}_{ij} - \mathbf{B}_{dj}\right|^2}}{\sqrt{\sum_{j=1}^{N}\left|\mathbf{B}_{dj}\right|^2}} \times 100 \qquad (14)$$

Where j is the sample number; $\mathbf{B}_{Ij}$ is the integration value with (13), $\mathbf{B}_{Dj}$ is the value calculated by the dipole model. We observe that the error decreases sharply when the distance increases. Especially, the error is 14.92% in the case of the distance 16mm, the same as the length of the magnet; 1.33% in 32mm, double of the magnet length; and 0.61% in 48mm, triple of the magnet length.

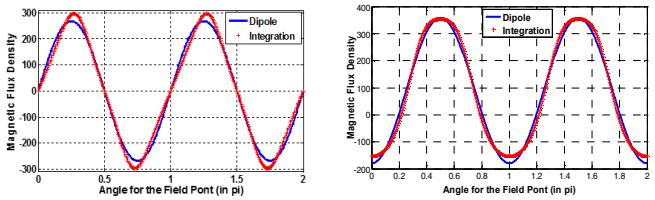

Fig. 6 Magnetic flux density components B_y and B_z in r=*20*mm (blue for diploe, red for integration)

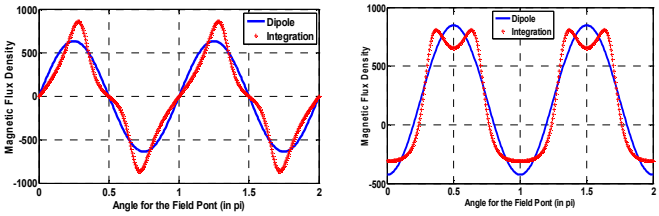

Fig.7 Magnetic flux density components B_y and B_z in r=15mm (blue for diploe, red for integration)

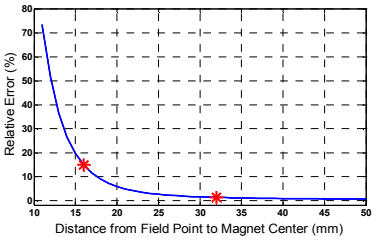

Fig.8 Relative errors of the integrations vs. those of dipole model

IV. Localization In Near Field

Fig.9 shows the flux density vector distribution around the ring magnet. Because it is symmetrical along the magnet's main axis, the density in a spatial point can be calculated by this 2D characteristic. The localization is to find the position and orientation parameters (*a, b, c, m, n, p*) as in Fig.1. However, from Fig.9, we know that magnet's flux distribution is 2 dimensional with respect to the magnet's center and the magnet's main (symmetrical) axis. Therefore, we can use some coordinate transforms to simplify the localization algorithm. Here, we propose a novel localization algorithm, and its procedure is listed as below.

a) Find the magnet's 2D density distribution with respect to the magnet's center (origin O) and mail axis (in z-axis) in advance. This can be completed by experiments or numerical calculations defined by a look-up table. For example in Fig.9, we build the lookup tables for 2D flux densities $\mathbf{B}$ corresponding to a spatial position (y, z)

$$\mathbf{B} = \bar{B}_y(y,z)\mathbf{j} + \bar{B}_z(y,z)\mathbf{k} \tag{15}$$

Where $\bar{B}_y(y,z)$ and $\bar{B}_z(y,z)$ are the y and z axis flux density components in y and z coordinates while x coordinate is fixed zero.

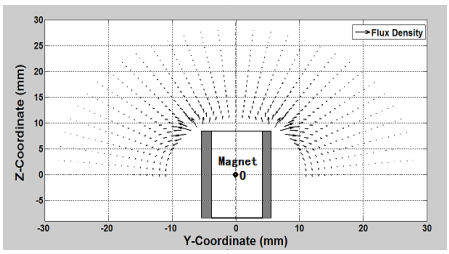

Fig.9 Magnetic flux density vector distribution (half plane) of ring magnet

b) We know that the magnetic field is symmetrical about the main axis (z-axis) of the magnet; so we can find the 3D (in x, y, z coordinates) magnetic flux density $\mathbf{B}_l$ (l=*1,2,...N*) with respect to the magnet's center through coordinate transform as

$$\begin{aligned}\mathbf{B}_l &= \bar{B}_{lx}\mathbf{i} + \bar{B}_{ly}\mathbf{j} + \bar{B}_{lz}\mathbf{k} \\ &= f_x(x,y,z)\mathbf{j} + f_y(x,y,z)\mathbf{j} + f_Z(x,y,z)\mathbf{k}\end{aligned} \tag{16}$$

c) As shown in Fig.10, assume that the spatial point A with coordinate (x, y, z) is on the plane AOC (point C is also on the plane XOY) that is perpendicular to plane XOY. We know that the magnetic flux vector $\mathbf{B}_l$ in point A is on this AOC plane because of the magnetic field symmetrical characteristic about the Z-axis. $\mathbf{B}_l$ can be decomposed as

$$\mathbf{B}_l = \mathbf{B}_r + \mathbf{B}_Z \tag{17}$$

Where $\mathbf{B}_r$ is the projection of $\mathbf{B}_l$ on the $\mathbf{r}$(=[x, y]) direction, and $\mathbf{B}_Z$ is projection of $\mathbf{B}_l$ on the Z-axis. With respect to Fig.9 and from equation (15) on the density lookup tables, we find

$$|\mathbf{B}_r| = \bar{B}_y(r,z) \tag{18}$$

$$|\mathbf{B}_z| = \bar{B}_z(r,z) \tag{19}$$

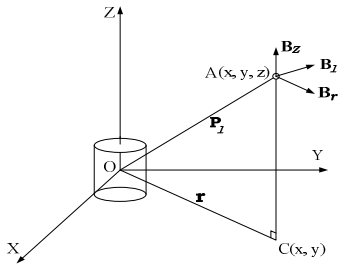

Fig.10 Magnetic density vector B_l (B_r+B_z) in plane AOC

Where $r = \sqrt{x^2 + y^2}$. Further, three orthogonal magnetic

flux components can be calculated as

$$\bar{B}_{1x} = f_x(x,y,z) = \bar{B}_y(r,z)\frac{x}{\sqrt{x^2+y^2}} \quad (20)$$

$$\bar{B}_{1y} = f_y(x,y,z) = \bar{B}_y(r,z)\frac{y}{\sqrt{x^2+y^2}} \quad (21)$$

$$\bar{B}_{1z} = f_z(x,y,z) = \bar{B}_z(r,z) \quad (22)$$

d) In the global coordinate system as in Fig.1, the magnetic flux densities (B_{1x} , B_{1y} , B_{1z}) in position (x_1, y_1, z_1) are measured by magnetic sensors; and initially the position and orientation parameters (*a, b, c, m, n, p*) are calculated by applying localization algorithm on the dipole model as (1)~(2).

e) Build a new coordinate system, defined as X'Y'Z', the magnet's coordinate system by using initial parameters (*a, b, c, m, n, p*) gotten in last step. In the new X'Y'Z' coordinate system, origin O' is in position (*a, b, c*) and Z'-axis is same as the magnet orientation (*m, n, p*); so the coordinate system is rotated from Z-axis to Z'-axis which is the same as (*m, n, p*). The rotation angle is

$$\theta = \cos^{-1}([0\ 0\ 1]\cdot[m\ n\ p]') = \cos^{-1}(p) \quad (23)$$

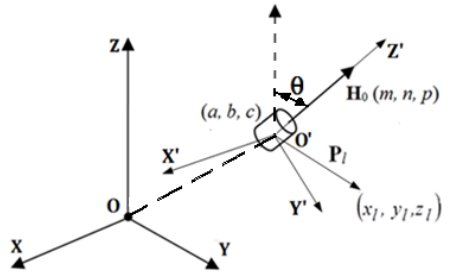

Fig.11 Coordinate system transform from the global system XYZ to magnet's system X'Y'Z'

Assume that the rotation is around the axis formed by the cross product of Z-axis and Z'-axis,

$$\mathbf{k}\times\mathbf{k}' = (0,\ 0,\ 1)\times(m,\ n,\ p)^T = (-n,\ m,\ 0)^T$$

Since $|\mathbf{k}\times\mathbf{k}'| = \sin\theta$, the unit vector of this axis is $\frac{(-n,\ m,\ 0)^T}{\sin\theta}$. Then, we get a rotation quaternion (q_0, q_x, q_y, q_z) with $q_0 = \cos(\frac{\theta}{2})$, $q_x = -n\frac{\sin(\frac{\theta}{2})}{\sin\theta}$, $q_y = m\frac{\sin(\frac{\theta}{2})}{\sin\theta}$, and $q_z = 0$. Then we get the rotation matrix

$$\mathbf{R} = \begin{pmatrix} q_0^2+q_x^2-q_y^2-q_z^2 & 2q_xq_y-2q_0q_z & 2q_xq_z+2q_0q_y \\ 2q_xq_y+2q_0q_z & q_0^2-q_x^2+q_y^2-q_z^2 & 2q_yq_z-2q_0q_x \\ 2q_xq_z-2q_0q_y & 2q_yq_z+2q_0q_x & q_0^2-q_x^2-q_y^2+q_z^2 \end{pmatrix} \quad (24)$$

f) In the new coordinate system X'Y'Z', calculate the positions of the sensors

$$\begin{bmatrix} x_1' \\ y_1' \\ z_1' \end{bmatrix} = \mathbf{R}^{-1}\bullet\begin{bmatrix} x_1-a \\ y_1-b \\ z_1-c \end{bmatrix} \quad (25)$$

and by using the flux density distribution relation (look up tables) in step a) and b), the corresponding flux densities are calculated as

$$\begin{bmatrix} \bar{B}_{1x} \\ \bar{B}_{1y} \\ \bar{B}_{1z} \end{bmatrix} = \begin{bmatrix} f_x(x_1', y_1', z_1') \\ f_y(x_1', y_1', z_1') \\ f_z(x_1', y_1', z_1') \end{bmatrix} \quad (26)$$

g) Transform [$\bar{B}_{1x}$ $\bar{B}_{1y}$ $\bar{B}_{1z}$]' to XYZ coordinate system by the rotation matrix **R**, and calculate the square difference to the measured sensor data (B_{1x} , B_{1y} , B_{1z})'.

$$\Delta B = \sum_{1=1}^{N}\left\| \begin{bmatrix} B_{1x} \\ B_{1y} \\ B_{1z} \end{bmatrix} - \mathbf{R}\bullet\begin{bmatrix} \bar{B}_{1x} \\ \bar{B}_{1y} \\ \bar{B}_{1z} \end{bmatrix} \right\|_2 \quad (27)$$

h) Minimization recursions (e.g., Matlab command *'lsqnonlin'*) can be applied to steps c) to f), to find the optimal position and orientation parameters (*a, b, c, m, n, p*) to minimize ΔB.

V. SIMULATIONS

5.1 An example

Here we present an example with the ring magnet (length=16mm, radius=6mm, and thickness=1.5mm) to show the performance of the algorithm. Assume that 5 triaxial magnetic sensors are in positions (-0.04, 0.12, 0), (0.12 0.04 0), (-0.04, 0.04, 0), (-0.12, -0.04, 0), and (0.04, -0.12, 0) in XYZ coordinate system (unit in meter), and the magnet's position and orientation are setup in (*a, b, c, m, n, p*)=(-0.0450, 0.1250, 0.0090, 0.5774, 0.5774, 0.5774). The algorithm runs as following:

a) By using near field model, the magnet's density distribution is computed by the integration on (13), which makes the 2D lookup table.

b) With the five sensor positions, the magnetic densities are calculated as

(-681.79, -126.55, 12.352); (0.0010, -0.1707, -0.1182); (-1.3717, 2.3181, -0.7700); (0.0816, 0.3350, -0.0973); (-0.0681, 0.0346, -0.0387).

The 1st data are very larger because this field point is much closer to the magnet. Applying the localization algorithm by the dipole model, (*a, b, c, m, n, p*) are obtained as

(-0.0471, 0.1244, 0.0081, 0.5416, 0.6155, 0.5726).

The differences relative to the setup magnet's position and orientation are

(-0.0021, -0.0006, -0.0009, -0.0358, 0.0381, -0.0048).

c) The rotation angle from Z-axis to Z'-axis is:

$$\theta = \cos^{-1}(p) = \cos^{-1}(0.5726) = 0.9611 \text{ (rad)}$$

The rotation quaternions are q_0 =0.8867; q_x=-0.3471; q_y =0.3054; q_z=0; and the rotation matrix is

$$\mathrm{R} = \begin{pmatrix} 0.8135 & -0.2120 & 0.5416 \\ -0.2120 & 0.7591 & 0.6155 \\ -0.5416 & -0.6155 & 0.5726 \end{pmatrix}$$

d) In X'Y'Z' coordinate system, the sensor positions are calculated to be

(0.0100, 0.0007, -0.0055); (0.1571, -0.0940, 0.0319); (0.0270, -0.0600, -0.0548); (-0.0212, -0.1038, -0.1473); (0.1260, -0.1985, -0.1099).

and by using the 2D magnet's density distribution, corresponding flux densities are calculated as

(-900.69, -250.96, 80.64); (-0.0168, -0.1688, -0.1185); (-1.3285, 2.6125, -0.7551); (0.0991, 0.3408, -0.0964); (-0.0698, 0.0426, -0.0385).

e) Calculate the square difference ΔB=106430.

f) By the recursions for the steps c) to f) to minimize ΔB, finally we get (a, b, c, m, n, p)=(-0.0450, 0.1250, 0.0090, 0.5774, 0.5774, 0.5774) and ΔB=2.9426×10^{-9}. The results are exactly the same as the presumed values.

5.2 De-noising capability

We also tested the algorithm for its de-noising capability by adding uniform noises to the sensor data. As shown in Fig.12, there are three sensor arrays with 5, 9, 16 sensors, we observe that the position errors increase with the noise level, but the total error level can be decreased if more sensors are applied for the sensor array. These simulation results validate the proposed algorithm is effective.

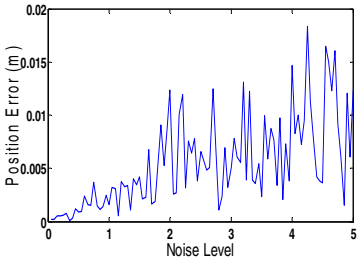

(a) 5 Sensors

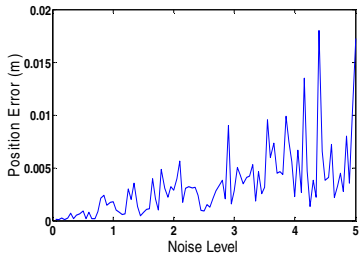

(b) 9 Sensors

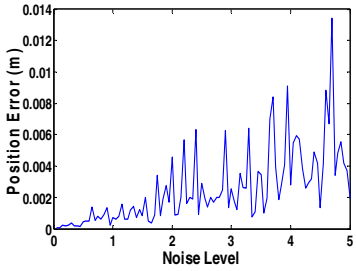

(c) 16 Sensors

Fig.12 Position errors via noise level in case of different number of sensors

VI. CONCLUSIONS

The near-field magnetic field distribution for a magnet is investigated comparing with the dipole model, which is simply symmetrical about the magnet's main axis. Based on this distribution and the localization results by the dipole model, the near-field localization algorithm is proposed, which minimizes the calculation error between the measured flux densities and those calculated from the spatial and rotation transforms from the global coordinate system to the magnet's coordinate system. Simulation results show that the proposed method can accurately to obtain the magnet's position and orientation in near-field.

ACKNOWLEDGMENT

This research was funded by National Natural Science Foundation of China (61273332), Ningbo Sc. & Tech. plan project (2016C50003, and Innovation Team 2014B82015), and the key technology project of Yibin(2017ZSF009-11).

REFERENCES

[1] C. Hu, M. Li, S. Song, W.A. Yang, R. Zhang, M. Q. H. Meng, "A Cubic 3-Axis Magnetic Sensor Array for Wirelessly Tracking Magnet Position and Orientation". IEEE Sensors Journal, 2010, 10(5): 903-913.

[2] C. D. Natali et al, "Real-time pose detection for magnetic medical devices." IEEE Transactions on Magnetics, 2013, 49 (7): 3524-3527.

[3] C. Hu, Y.P. Ren, X.H. You, W.A. Yang, S. Song, S. Xiang, X.Q. He, Z.H. Zhang, and M. Q.-H. Meng, "Locating Intra-Body Capsule Object by Three-Magnet Sensing System"; IEEE Sensors Journal ，2016, 16(13):5167~5178.

[4] X.D. Wu et al, "Wearable magnetic locating and tracking system for MEMS medical capsule"; Sensors and Actuators A: Physical, 2008, 141:432–439.

[5] E. Stathopoulos, V. Schlageter, B. Meyrat, Y. de Ribaupierre, and P. Kucera, "Magnetic pill tracking: A novel non-invasive tool for investigation of human digestive motility," Neurogastroenterol. Motility, 2005, 17(1): 54–148.

[6] T. D. Than et al; "A Review of Localization Systems for Robotic Endoscopic Capsule"; IEEE Trans. On Biomedical Engineering, 2012, 59(9):2387-2399.

[7] C. Hu, M. Q.-H. Meng, M. Mandal; "A Linear Algorithm for Tracing Magnet's Position and Orientation by using Three-Axis Magnetic Sensors". IEEE Transactions on Magnetics, 2007, 43(12): 4096-4101.

[8] C. Hu, M. Q. Meng, and M. Mandal, "Efficient magnetic localization and orientation technique for capsule endoscopy," Int. J. Inf. Acquisition. 2005, 2(1):23–36.

[9] Y.P. Ren, et al; "Magnetic Dipole Model in the Near-field"; Proc. of the 2015 IEEE International Conference on Information and Automation Lijing, China, August 2015. Pp:1085~1089.